THE BELL SYSTEM TECHNICAL JOURNAL
Vol. 59, No. 5, May–June 1980
Printed in U.S.A.

The EL2 Electret Transmitter: Technology Development

By S. P. KHANNA and R. L. REMKE

(Manuscript received November 26, 1979)

The design and development of a new telephone transmitter based on the electret properties of fluoroplastic polymer films required the implementation of new technologies consistent with manufacturing and reliability goals. Techniques for continuously charging and metallizing such films have been evaluated. Precision molding and metallization of plastic parts critical to the design were also studied. The embodiment of the electronics into the microphone design was accomplished via hybrid integrated-circuit technologies. In each case, process capability studies and reliability studies have provided a firm basis for introduction of these new technologies.

I. INTRODUCTION

The first electrets were made by the Japanese physicist Eguchi in 1919 using carnauba wax.[1] Subsequently, other thick organic waxes were used in early electret microphones such as the World War II Japanese field equipment and the commercially offered "No-voltage Velotron."[2] However, these electrets suffered from poor electrical stability. Fluoroplastic polymer materials such as Teflon* have excellent electrical characteristics even after exposure to high temperature and high humidity conditions. The availability of such materials, along with a better understanding of the technology, has given rise to reliable transducers based on electrets.

Polymer film electret transducers, developed by G. M. Sessler and J. E. West of Bell Laboratories in the early 1960s,[3] have many technical advantages. For a given acoustic input, electret microphones generate the highest electrical signal of any type of microphone except the carbon transmitter. The flatter response of an electret microphone

* Registered trademark of E. I. DuPont de Nemours.

means frequency shaping is easier to obtain. In addition, electrets have extremely low sensitivities to external mechanical vibration and electromagnetic signals. They have some advantages even over air-condenser and ceramic microphones. An air-condenser microphone requires a high polarizing voltage (up to 200 volts or higher) applied across the narrow gap between the diaphragm and the back-plate. In contrast, there is no free electrostatic charge in an electret transducer, as the electret charge is permanently trapped in the polymer diaphragm film.

II. TRANSMITTER DESIGN

An electret transducer is basically a variable capacitance-type transducer as shown in Fig. 1. A charged polymer film, which is metallized on one side, serves as the diaphragm. It is supported adjacent to a stationary electrode surface on small support ridges creating an effective air gap. The charge on the electret film creates an electric field across the air gap. Sound waves impinging on the diaphragm modulate the electric field and generate a corresponding voltage drop across a load impedance.

The embodiment of these principles into the EL2 electret microphone is discussed in a companion paper.[4] The various components of this design are shown in Fig. 2 for reference. The electret diaphragm, having one surface metallized, is tensioned across the ribs of the backplate with the metallized surface facing away from the backplate and, while so tensioned, the ends of the diaphragm are clamped against the backplate by a conductive clamping plate that makes electrical contact with the diaphragm. The conductive clamping plate is held in place by a conductive spring clip that wraps around the foregoing assembly and presses the clamping plate and the pre-amplifier substrate towards each other. This spring provides the clamping force necessary to retain the desired tension on the diaphragm and at the same time secures the substrate in the recessed section under the backplate. The spring clip, further, includes a terminal that mates with

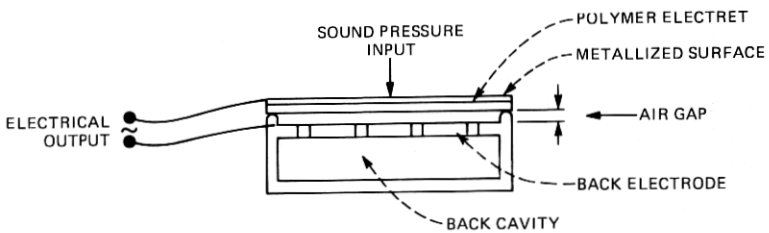

Fig. 1—Electret microphone.

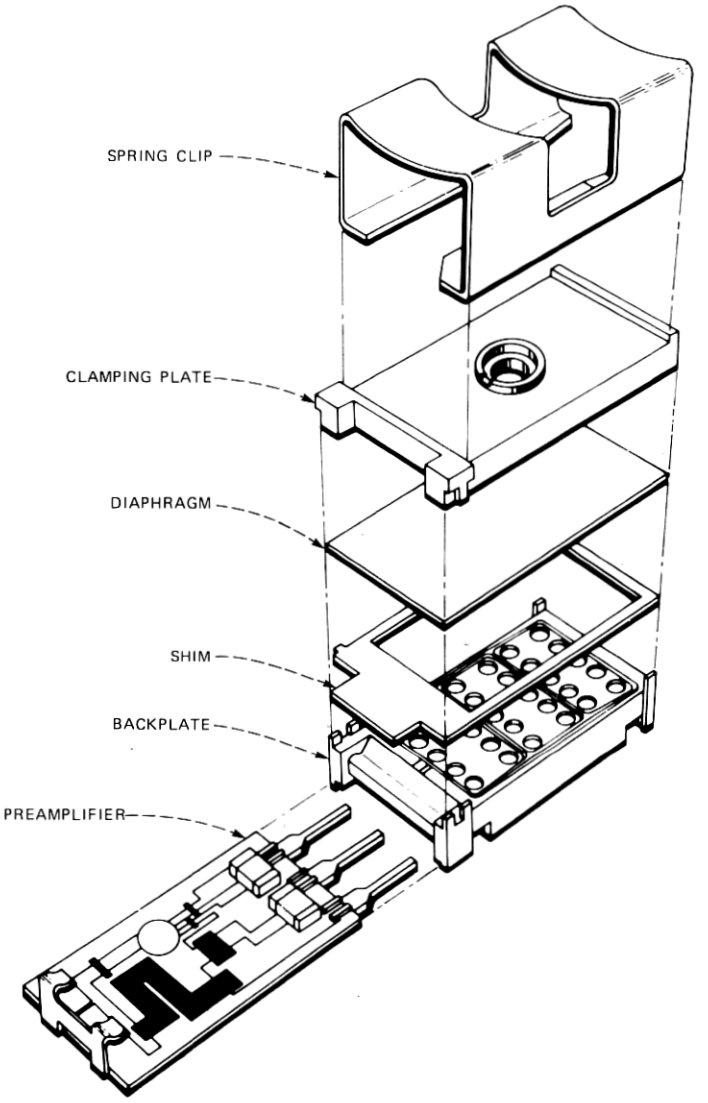

Fig. 2—EL2 subassembly—exploded view.

the ground lead of the preamplifier and, together with the conductive clamping plate, provides a conductive path to the ground for the conductive surface of the diaphragm. Some basic physical design parameters are shown in Table I.

The implementation of the EL2 design required the development of

Table I—Design parameters

Electret Material	Polytetrafluoroethylene (PTFE)
Electret diaphragm film thickness (d)	25.4 μm
Dielectric constant of PTFE (ϵ)	2.0
Total effective diaphragm area (A)	8×10^{-5} m^2/cell
Number of cells	3
Electret: Equivalent surface charge	13.9×10^{-5} C/m^2
Equivalent voltage	200V
Electret film tension	25 nt/m
Air gap	36 μm
Rear chamber volume	3×10^{-7} m^3

new technologies for metallizing and charging the electret diaphragm. These processes were evaluated with respect to both manufacturability and reliability. The use of plastic parts for both the clamping plate and the backplate required development of precision molding to control such parameters as air gap spacing and the ability to metallize these parts for their electrode and conductor functions. Finally, the EL2 design also embodied an impedance conversion preamplifier in the form of a hybrid integrated circuit.

III. NEW TECHNOLOGIES

3.1 Metallization of the electret diaphragm

The processes for deposition of a metal film onto the electret diaphragm must meet several objectives. First is an adequate adhesion between the metal and the polytetrafluoroethylene (PTFE)[5] diaphragm. Second, the processes cannot adversely affect the electrical characteristics of the diaphragm, and, third, the processes must be economical. The choice of gold for the metal film presented the challenge of achieving adherence of the gold to the PTFE film. The strength of gold-PTFE joints using an untreated PTFE surface is weak due to the presence of surface regions of low mechanical strength. Some surface treatments, like chemical etching of surface and CASING (Cross-linking by Activated Species of Inert Gases) technique prior to the evaporation process, have been used for increasing the strength of the bond between the polymer and deposited gold.[6,7] The adhesive joints formed between PTFE thus treated and gold can be as strong as the bulk strength of the PTFE. The surface treatments obviously modify the surface regions and strengthen the boundary layers. Sputter deposition of gold onto the PTFE foil can also give increased adherence. These processes improve the adhesive joint strength but also degrade the electrical properties of PTFE.

Roberts, Ryan, Schonhorn, et al[8] developed a new process for

increasing the bond strength of gold to Teflon FEP. This process does not affect the electret behavior of the virgin polymer material. A layer of aluminum is deposited on the foil by evaporation and later removed by etching in a dilute solution of sodium hydroxide. Gold is then vacuum-deposited on this etched foil. The tensile shear strength of this composite is in excess of 80 kgm/cm^2. This is quite an improvement over the tensile strength of 0.070 kgm/cm^2 of gold on the untreated FEP. X-ray photo-electron (ESCA) spectra suggest that the modified wetting angle and enhanced strengths can be attributed in part to the existence of a layer of oxygen-containing hydrocarbon material on the surfaces of the aluminum-treated Teflon FEP.

The process developed for metallizing the diaphragm used in the EL2 microphone consists of sequentially vacuum-depositing a thin layer of titanium followed by the gold metal film to the desired thickness.[9] The titanium layer provides the adherence of the gold to the PTFE film. Use of titanium or other reactive metals as an undercoating has been used in other applications to obtain adhesion of gold to glass or ceramic substrates.[10] This approach has now been successful for fluorocarbon films such as FEP, ETFE, CTFE, and PTFE. The tensile shear strength for FEP Teflon metallized with 0.02 μm of titanium and 0.20 μm of gold was found to be 140 kgm/cm^2.[11] Charging and equivalent voltage decay studies indicate no adverse effects due to the metal system. Moreover, the ability to continuously metallize the diaphragm film in one vacuum cycle reduces the complexity of the manufacturing process in comparison with previously described methods.

To fully characterize the metallization process, a vacuum deposition system was developed, capable of handling film lengths of up to 100 feet. This system is shown in Fig. 3. The film is transferred across two sources which are evaporating the titanium and gold metals. Shielding between the two sources minimizes cross-contaminations of the metal films. Water cooling of the fixtures minimizes the surface heating of the PTFE during evaporation to less than 50°C. The film transfer mechanism consists of supply and take-up reels, capstan rollers, and a motor with a tachometer feedback speed control. Braking and tensioning the foil was provided by pressure from an adjustable spring-loaded drag plate on the shaft of the supply roll. The motor torque was transferred to the shaft of the take-up spool with the help of a rotary feed-through and a set of gears. All the rollers were set in self-aligning bearings to maintain parallelism among the rollers. This was found to be necessary for the proper tracking of the limp and elastic PTFE film.

Titanium is evaporated using a bank of resistively heated filaments. Gold is evaporated from a crucible using RF induction heating. The crucible contains a sufficient quantity of gold to continuously evaporate onto a 100-ft length of PTFE film. The choice of the sources was

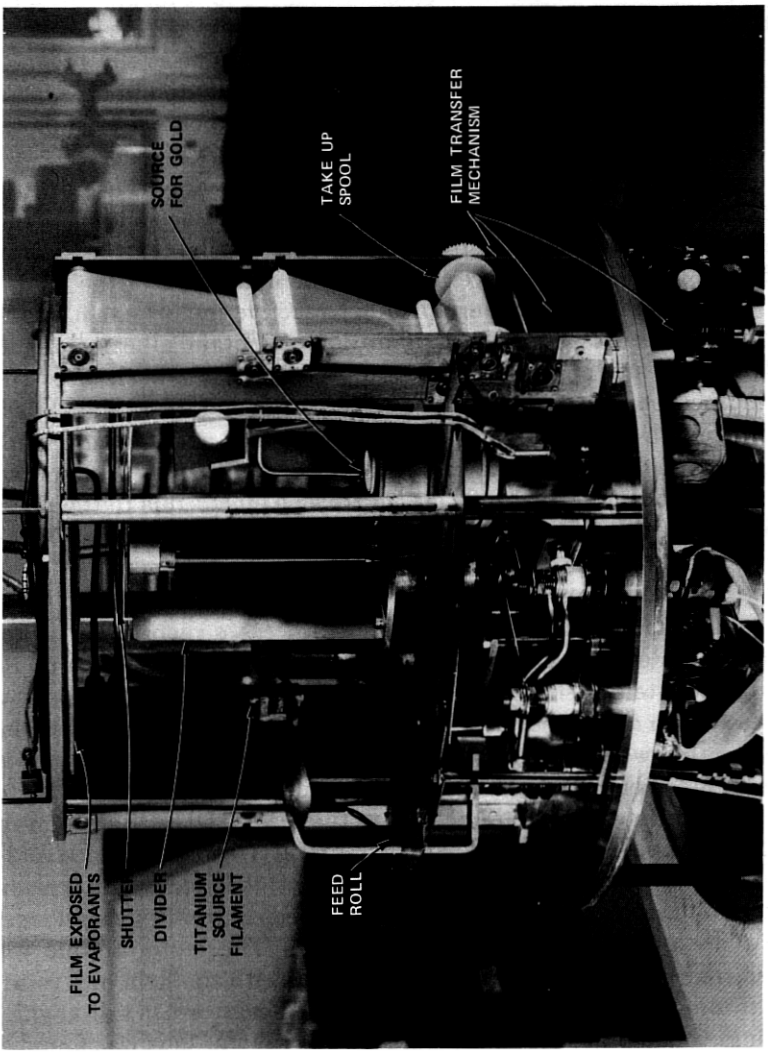

Fig. 3—Dual metallization system.

dictated by the need to control the deposition rates of the two metal depositions over the 10 to 15 minutes required to move the PTFE film past the sources. A quartz crystal thickness monitor is used for controlling the titanium thickness. For the gold, the rate was controlled by the power applied.

Various deposition processes were studied to determine the effect on electrical characteristics of the PTFE films as well as metal-PTFE adherence. Induction-heated evaporation was compared to sputtering and electron beam evaporation. The effect of these deposition processes on the equivalent voltage decay (see Section 3.2) was monitored by isothermal equivalent voltage decay measurements. Figure 4 demonstrates these effects. Here, three samples of PTFE, metallized by each of the methods and then corona-charged to a given equivalent voltage, are annealed at 150°C. The change in equivalent voltage during the thermal annealing can be seen to depend in part on the mode of deposition of the metal film. It is hypothesized that either ion or X-ray bombardment during deposition alters the intrinsic conductivity of the PTFE films causing the equivalent voltage to decay rapidly.[12] Such bombardment can occur during sputtering or electron beam evaporation. The PTFE films coated with gold using the RF induction heating technique give superior equivalent voltage decay characteristics.

The titanium-gold metal system was also tested under various acceleration conditions to evaluate long-term reliability of the gold-PTFE joint strength. Tensile shear strengths were measured for PTFE films metallized on both sides. The samples were epoxy-bonded to aluminum strips, maintaining a 6.54-cm^2 overlap. The joint strengths

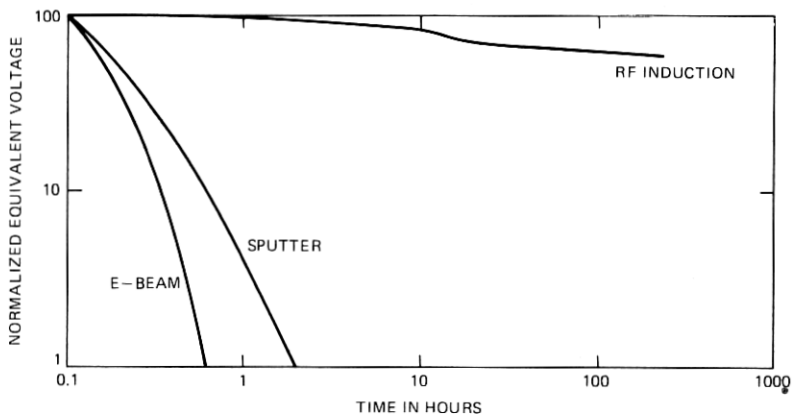

Fig. 4—Equivalent voltage decay characteristics of metallized PTFE film.

were tested per ASTM 1002-64 prior to and after accelerated aging. No adverse long-term effects were found. The results of the tests are summarized in Fig. 5.

3.2 Charging of the electret diaphragm

Electret material can be charged by numerous techniques including the simultaneous applications of electric field and heat,[3] corona discharge,[13,14] breakdown methods,[15] electron bombardment,[16] and electron injection.[17] A relatively simple charging technique suitable for high volume production consists of using a blade charger[18] as shown in Fig. 6. The metallized PTFE film is fed from a supply reel with the metallized side in contact with the ground roller. The film is then drawn over a gold-plated blade and rolled up on the take-up reel. The blade is kept at a high potential, and the current into the ground roller is measured with an electrometer. The charge injected into the electret film is monitored by measuring the equivalent voltage of the film using an electrostatic voltmeter. The equivalent voltage is given by

$$V_e = \frac{1}{\varepsilon_0 \varepsilon} \int_0^d xp(x)\, dx, \tag{1}$$

where $p(x)$ is the charge/volume, x is the displacement, d is the film thickness, ε_0 is the permittivity of free space, and ε is the dielectric constant of the electret material. For corona charging, the integral of

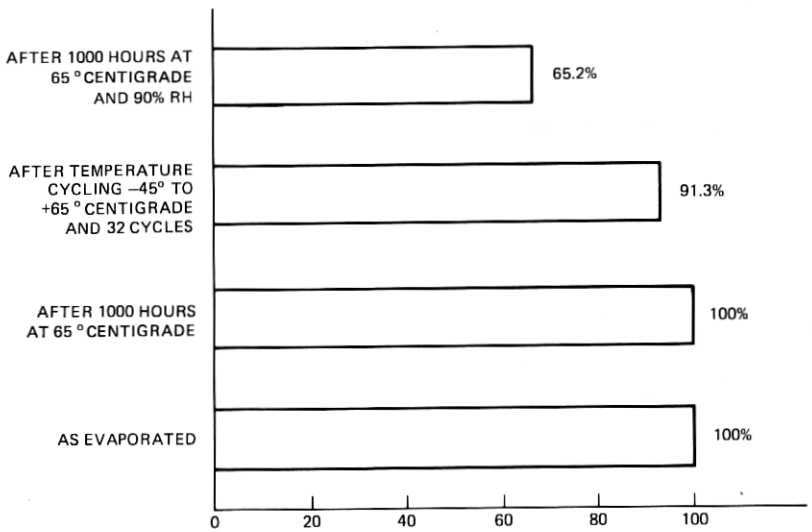

Fig. 5—Effect of accelerated aging on gold-PTFE joint strength.

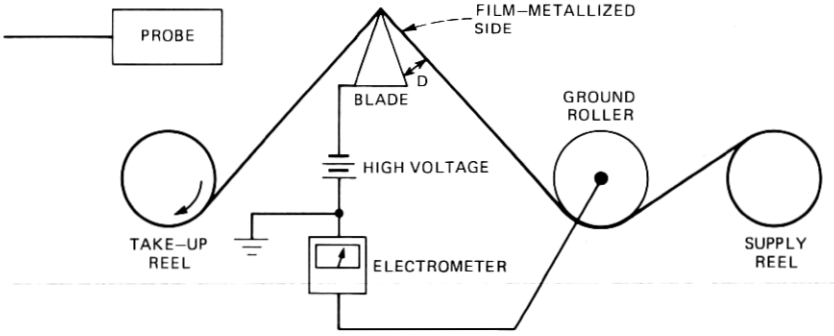

Fig. 6—The blade charger.

the charge density can be approximated by a surface charge density since the charge is very near the free surface. Therefore,

$$V_e = \frac{d\sigma_e}{\varepsilon_0 \varepsilon}, \tag{2}$$

where σ_e is the surface charge density (in C/cm^2). This system allows an entire roll of film to be charged at rates of up to 6 cm/s.

The charging of the electret film on the blade charger can be described by an air breakdown or corona discharge model. As the film approaches the blade, the electric field in the air gap causes the air to break down. This air breakdown creates charged carriers which are driven by the electric field toward either the blade or the electret film. For breakdown to occur, the voltage across the air gap must exceed that for breakdown at a particular gap width. Two aspects must be considered. First, the voltage across the gap must be determined with respect to the applied voltage. Since we have in essence a two-dielectric capacitor arrangement, the voltage across the gap V_g is given by

$$V_g = (V - V_e) \cdot (D/((d/\varepsilon) + D)), \tag{3}$$

where V is the applied voltage and D is the air gap width. Second, the voltage across the air gap must exceed the breakdown voltage V_b given by[19]

$$V_b = 312 + 6.2D, \tag{4}$$

where V_b is in volts and D is in microns. As the film moves, this gap width for a particular spot on the film decreases as the spot approaches the contacting edge of the blade. For corona-charging to take place at a particular D,

$$V_g > V_b \quad \text{or} \quad V_g - V_b > 0.$$

This yields

$$(V - V_e)(D/((d/\varepsilon) + D)) - 312 - 6.2D > 0. \quad (5)$$

Breakdown will occur in the blade charger when D decreases to a value such that (5) is satisfied. This value of D is determined by setting eq. (5) to zero and solving. Two values of D are obtained, and breakdown will first occur at the highest D in the blade charger. This first breakdown results in the film charging to some small level assuming that V_e is initially zero. As D is reduced further, the film will charge more, and V_e will increase again. This process will continue as D decreases until the value of V_e increases above that for which the equation can never be greater than zero for any value of D. Mathematically, this is the point where there is only one value of D for eq. (5), or where $b^2 = 4ac$ if the equation is written in the standard quadratic form. This yields the relation between V_e and V at extinction,

$$V_e = V - 6.2d/\varepsilon - 88.0\sqrt{d/\varepsilon} - 312, \quad (6)$$

where V_e is in volts and d is in microns. At this point, corona charging stops and the equivalent voltage across the film is that measured after charging. This quasi-static approach to the charging mechanism assumes that the charging time is much less than the film speed. This is justified, since the film-charging level is not dependent on the film speed over the range investigated.

The above analysis predicts equivalent voltage versus applied voltage curves like those shown in Fig. 7 for two thicknesses of PTFE film. The actual experimental results are also shown in the same figure. The general shapes of the curves are very similar, with a flat "no-charging" region followed by a "charging" region where the equivalent voltage increases linearly with applied voltage. It is noted that the experimental and theoretical equivalent voltage slopes are very similar, although the actual experimental equivalent voltages are larger than those predicted from theory. This deviation of the experimental and theoretical curves is probably due to the oversimplification of eq. (4) for small air gaps.

3.2.1 Accelerated equivalent voltage decay studies

Important in any practical use of electrets is the equivalent voltage decay time and therefore device lifetime. Since equivalent voltage decay times are of the order of years for many electret materials, accelerated tests[20] are used where the driving force is elevated temperature. Two types of tests are used to study equivalent voltage decay, open-circuit thermally stimulated current measurements (open-circuit TSCs), and open-circuit isothermal equivalent voltage decay measurements. Open-circuit TSCs measure equivalent voltage changes

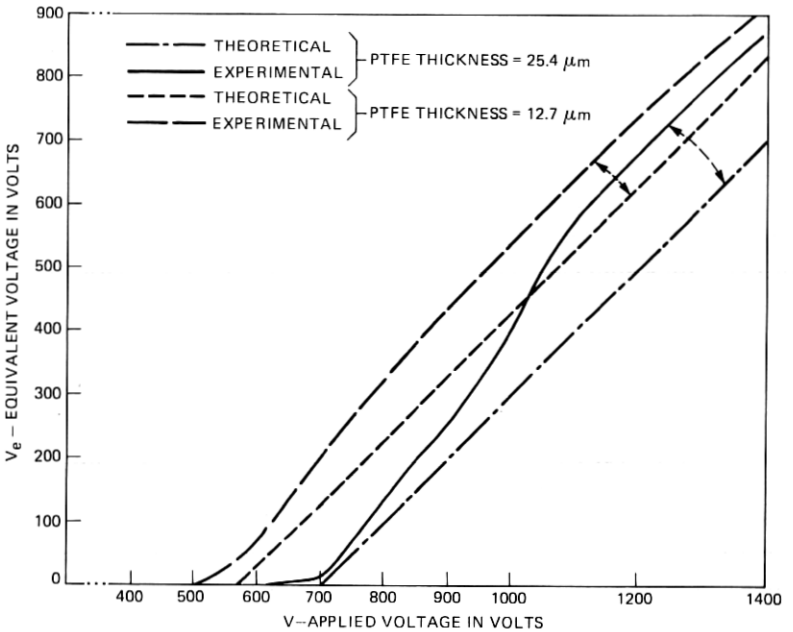

Fig. 7—Electret film equivalent voltage vs the applied voltage for the blade charger.

as the temperature is linearly increased. Isothermal equivalent voltage decay measurements monitor the change of the equivalent voltage at elevated temperatures as a function of time. These techniques offer different perspectives in studying equivalent voltage decay.

The open-circuit TSC measurements were made using the experimental setup shown in Fig. 8. The top electrode (7.2-cm diameter) was supported 0.5 cm above the nonmetallized side of the electret, while

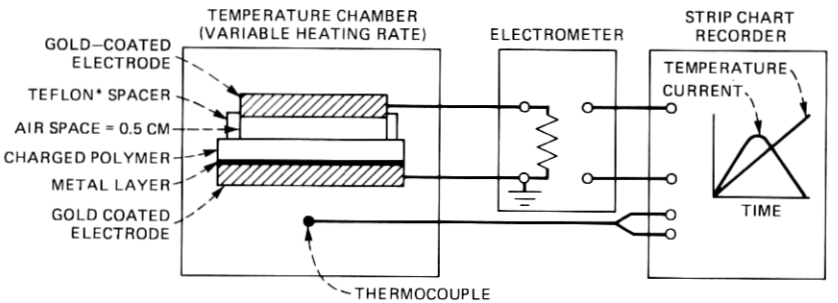

*TRADEMARK OF E.I. DUPONT DE NEMOURS

Fig. 8—The open-circuit TSC measurement system.

the metallized side made electrical contact with the bottom electrode. The temperature was raised at 1°C/min, and the outputs were recorded. Before any measurements were made, open-circuit TSCs were made on uncharged films until no current was measured. This assured that any charge on the apparatus, electrodes, etc., had dissipated. The results for corona-charged PTFE are shown in Fig. 9. The measured current indicates changes in the equivalent voltage, while peaks indicate particular mechanisms. These TSC measurements also can be used for fast evaluations of changes in the manufacturing processes.

The isothermal PTFE decay studies were performed at various temperatures with the electrets held in an open-circuit condition. The electrets were kept in metal containers so as to reduce charge decay by charge compensation from ions in the heated oven.[21] Typical results for different temperatures are shown in Fig. 10. It is seen that increasing the temperature increases the equivalent voltage decay rate. Decay studies at several temperatures and for longer times can be used to extrapolate performance at 25°C.[22] Figure 11 shows the times required at various temperatures for the equivalent voltage to decay 10 percent. Such a series of curves were used to estimate the room temperature decay as given in Fig. 12. This figure also shows actual decay measurements made over the course of five years.

3.3 Clamping plate and backplate processing

The microphone sensitivity and frequency response are dependent on the joint effects of the diaphragm tension and charge, front and back acoustic chamber volumes, and the air gap between diaphragm and back electrode surface.[4] The clamping plate and the back plate define the two acoustic chambers and air gap height as well as maintain

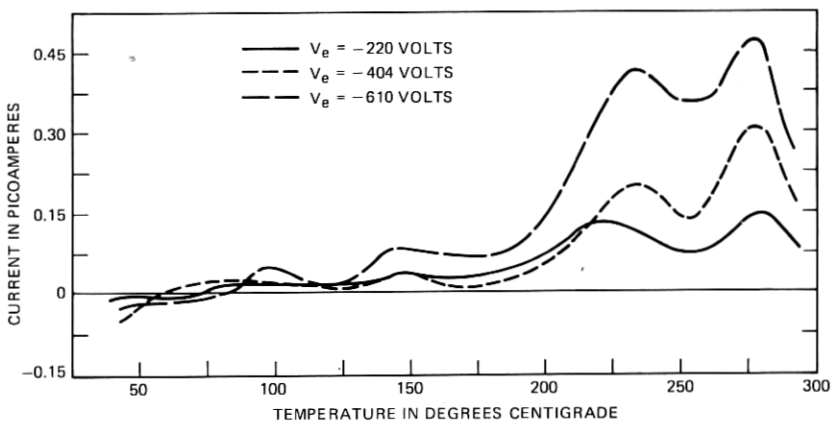

Fig. 9—Open-circuit TSCs for corona-charged PTFE.

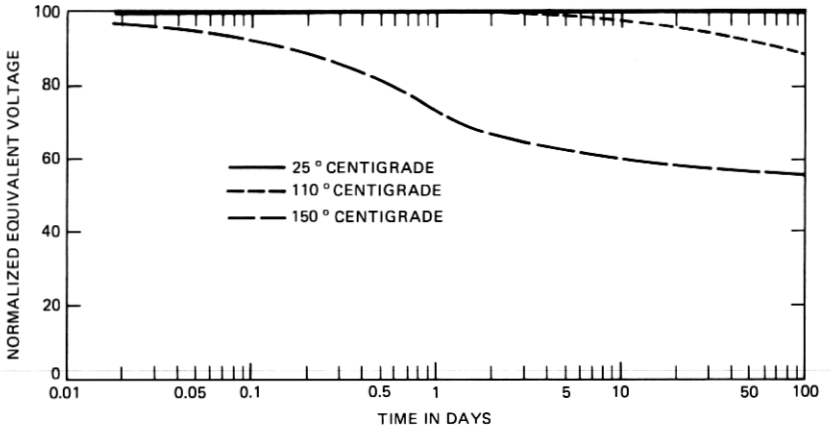

Fig. 10—Isothermal equivalent voltage decay at 25°C, 110°C, and 150°C for corona-charged PTFE.

the tension on the film (Fig. 13). The two plates must not only meet dimensional requirements but also be capable of being metallized. A series of process capability studies were performed to insure that both the molding and metallization processes were compatible.

The clamping plate is fabricated from acrylonitrile-butadiene-styrene copolymer (ABS) using standard injection molding techniques.

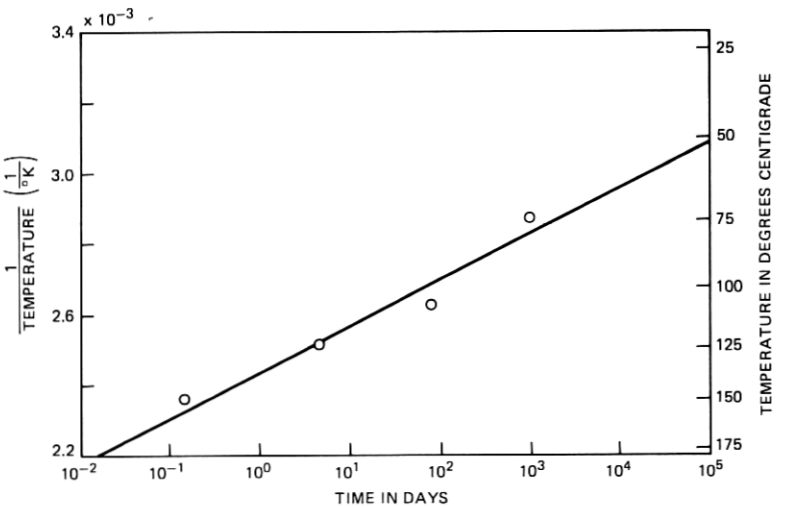

Fig. 11—1/temperature vs time for equivalent voltage to decay 10 percent for corona-charged PTFE.

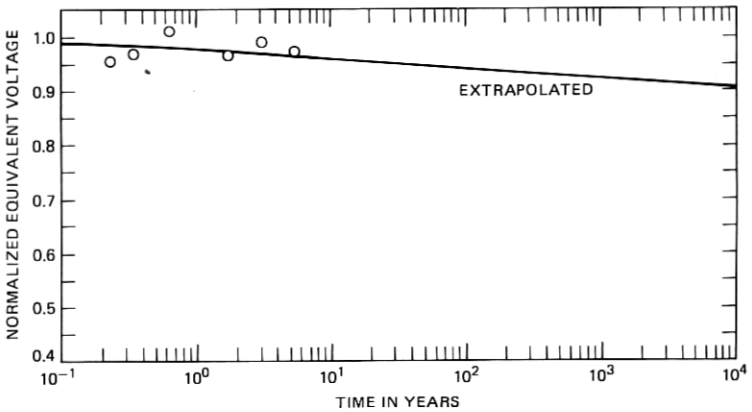

Fig. 12—Extrapolated electret equivalent voltage at 25°C vs time.

These parts are then plated using a copper or nickel underplate followed by a soft gold plate. Molding parameters such as stock and mold temperatures, injection rate, and pressure were varied over a range of processing conditions to evaluate the platability of the parts. The plating processes evaluated were those of commercial suppliers.

The first step in plating the parts consists of cleaning and etching the ABS surface. The etching step removes the surface butadiene to provide sites for the precious metal catalyst also used in the pretreatment stage. Good platable plastic parts require a dispersion of this butadiene over the entire surface. Under ideal conditions, the part would be molded with no stresses and the butadiene dispersed uniformly. In practice, the molding conditions were varied to minimize stresses and maximize the butadiene dispersion.

The molding process studies indicated the need to use the slowest injection rate and lowest injection pressure consistent with the dimensional requirements of the part. Given a successful pretreatment (and proper molding), the parts could be plated using standard electroless copper or nickel plating followed by electroplating of the underplate and gold. Evaluation of the parts was made on the basis of appearance (lack of voids, blistering, etc.), and adherence. A tape test for adherence was used for these studies with the intent of maintaining the test as a process connrol.

Accelerated testing of these parts was also conducted as part of the process capability studies. The tests consisted of high temperature aging (65°C), high temperature and high humidity (65°C/90% RH) storage, and temperatures cycling (65°C to −45°C). The most stringent requirement was the temperature and humidity test for 1000 hours with no degradation of the plated surface. During this test, failures

were found on one of the two types of ABS resins evaluated, and parts with an underplate thickness of less than 2.54 μm. No significant effect was observed for the variations in either molding or plating process parameters. As a result of the process evaluation studies for both molding and plating, a process capability was established for the clamping plate which will give good field performance.

The backplate was metallized by evaporation techniques. Here, selective metallization through a mechanical mask defined the backplate electrode and contact area. The sequential deposition of titanium and gold was used to achieve adherence of the gold film to the plastic backplate. Both the clamping plate and backplate were molded from the same grade of ABS material so as to have a similar expansion coefficient. This coefficient also approximates that of the metallized PTFE electret film.

In the microphone, the backplate defines the three active capacitor cells, as well as the air gap via the molded ribs (Fig. 13). Molding parameters and sufficient process windows were of concern to meet

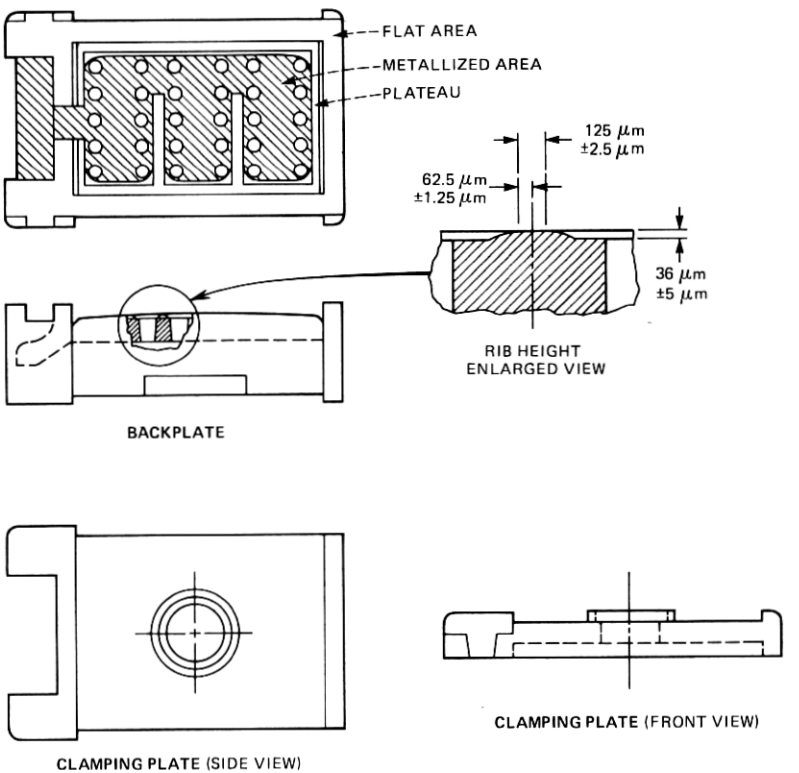

Fig. 13—Backplate and clamping plate.

the rib height requirements of 36 ± 5 μm as well as the flatness requirements in each cell of the backplate (i.e., absence of any sink marks). Process capability studies, conducted through a range of conditions, indicated the ability to tightly and routinely control the rib heights. However, tighter control over the injection rate and pressure was needed to control the sink in the plateau area. The optimum injection rate and pressure to control rib heights and flatness of the backplate are opposite that for the clamping plate; consequently, higher stresses in the backplate are to be expected.

This impacts on the metallization process, since exposure to excessive temperatures during metallization will cause the parts to warp and be unusable. Standard vacuum deposition techniques were used to selectively metallize the parts. Care was used in reducing the temperature seen by the parts during metallization. Both electron beam and filament sources were used successfully, provided the time of evaporation was limited.

3.4 Impedance conversion pre-amplifier

The electret microphone, in the presence of an acoustic field, performs as a voltage source in series with a small capacitor (see Section II). This electret microphone cartridge has an impedance of about 100 megohms at 100 Hz. To provide an impedance transformation to a nominal output impedance of 1 kilohm, an impedance conversion preamplifier based on hybrid technology was designed into the back cavity of the EL2 microphone. This circuit is shown schematically in Fig. 14 and consists of a JFET source follower stage. It has two resistors, R_1 = 100 megohms and R_2 = 10 kilohms. Two capacitors across the output leads provide protection from radio frequency interference. Note in Fig. 2 that the hybrid circuit essentially defines the back surface of the rear acoustic chamber of the microphone.

This circuit can be fabricated using either thick-film or thin-film

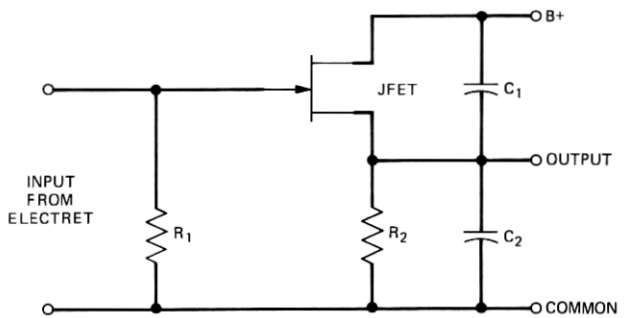

Fig. 14—Electret preamplifier circuit.

techniques. For thick film, the two capacitors are discrete appliqued capacitors, while for thin film, the large value resistor (R_1 = 100 megohms) is an appliqued device. Note also that, in addition to the three external leads soldered to the circuit, a contact spring is attached. This contact spring mates with the backplate to provide a pressure contact between the circuit and the back electrode of the electret. Interconnection of the metallized diaphragm is made through the clamp plate and spring clip and soldered to the circuit lead.

IV. CONCLUSIONS

The design and implementation of the electret microphone required the development and evaluation of several new technologies. Processes have been developed for continuously charging and metallizing the PTFE film in a uniform and consistent manner. The key parameters required for precision molding and metallization of the plastic parts used in the design have been identified, again to provide ease of manufacture. Finally, the technologies needed to incorporate the electronics into the physical design of the microphone have been implemented. Thus, the goal of implementing new technologies, consistent with manufacturability and reliability consideration, and compatible with the physical design and analysis of the electret microphone has been met. Moreover, the process capability studies accompanying this effort have proven invaluable in the introduction of these technologies into manufacture.

V. ACKNOWLEDGMENT

The authors would like to take this opportunity to thank the coworkers whose aid and contributions made this work possible. Special thanks are offered to L. H. Drexler who molded ABS plates, D. J. Wallace who did the plating of clamping plates, and S. M. Wecker who did initial charging and equivalent voltage decay studies. Finally we are grateful to D. G. Muth for fruitful discussions throughout the development of this project.

REFERENCES

1. M. Eguchi, "On Dielectric Polarization," Proc. Phys. Math. Soc., Japan, *1* (1919), pp. 326–331.
2. Bogen Catalogue (1939), p. 16. See also W. A. Bruno, U. S. Patent 2,284,039, May 26, 1942.
3. G. M. Sessler and J. E. West, "Self-Biased Condenser Microphone with High Capacitance," J. Acous. Soc. Amer., *34,* Number 11 (November 1962).
4. J. C. Baumhauer, Jr. and A. M. Brzezinski, "The EL2 Electret Transmitter: Analytical Modeling, Optimization, and Design," B.S.T.J., *58,* No. 7 (September 1979), pp. 1557–1578.
5. The Carborundum Company, Dilectrix Division, Farmingdale, N.Y.
6. G. M. Sessler, J. E. West, F. W. Ryan, and H. Schonhorn, "Increase of Gold-Teflon

FEP Joint Strength by Electron Bombardment," J. Appl. Polym. Sci., *17* (1973), pp. 3199–3209.
7. H. Schonhorn and R. H. Hansen, "Surface Treatment of Polymers for Adhesive Bonding," J. Appl. Polym. Sci., *11* (1967), pp. 1461.
8. R. F. Roberts, F. W. Ryan, H. Schonhorn, G. M. Sessler, and J. E. West, "Increase of Gold-Teflon FEP Joint Strength by Removal of Deposited Aluminum Prior to Gold Deposition for Electret Applications," J. Appl. Polym. Sci., *20,* No. 1 (1976), pp. 255–265.
9. S. P. Khanna, "Technique for Fabrication of Foil Electret," U. S. Patent 3,991,321, November 9, 1976.
10. R. W. Berry, P. M. Hall, and M. T. Harris, *Thin Film Technology*, New York: Van Nostrand Reinhold, 1968, p. 586.
11. H. Schonhorn and F. W. Ryan, private communication.
12. S. P. Khanna, unpublished work.
13. K. W. Tyler, J. H. Webb, and W. C. York, "Measurements of Electrical Polarization in Thin Dielectric Materials," J. Appl. Phys., *26,* No. 1 (January 1955), pp. 61–68.
14. R. A. Creswell and M. M. Perlman, "Thermal Currents from Corona Charged Mylar," J. Appl. Phys., *41,* No. 6 (May 1970), pp. 2365–2375.
15. G. M. Sessler and J. E. West, "Production of High Quasipermanent Charge Densities on Polymer Foils by Application of Breakdown Fields," J. Appl. Phys., *43,* No. 3 (March 1972), pp. 922–926.
16. G. M. Sessler and J. E. West, "Charging of Polymer Foils with Monoenergetic Low-Energy Beams," Appl. Phys. Lett., *17,* No. 12 (December 15, 1970), pp. 507–508.
17. J. P. Cross and R. Blake, "Charge Trapping Mechanisms in Foil Electrets," *Electrets, Charge Storage and Transport in Dielectrics*, Princeton, N. J.: Electrochemical Society, 1973, pp. 300–304.
18. S. M. Wecker, "Polymer Film Electrets, Charging, Charge Decay, and Applications," Proc. 35th Annual Technical Conf., Society Plastics Engrs., Montreal, 1977, pp. 370–372.
19. R. M. Schaffert, *Electrophotography*, London: Focal Press, 1975, p. 523.
20. J. Van Turnhout, *Thermally Stimulated Discharge of Polymer Electrets*, New York: Elsevier, 1975, pp. 5–7.
21. E. W. Anderson, L. L. Blyler, Jr., G. E. Johnson and G. L. Link, "Electret Stability in the Presence of Ions," *Electrets, Charge Storage and Transport in Dielectrics*, Princeton, N. J.: Electrochemical Society, 1973, pp. 424–435.
22. R. E. Collins, "Production and Application of Long Life Electrets," Proc. IEEE, *34* (October 1979), pp. 381–390.